Localization via Taylor Series Approximation for UWB based Human Motion Tracking

Zemene W. Mekonnen and Armin Wittneben
Communication Technology Laboratory, ETH Zurich, 8092 Zurich, Switzerland
{mekonnen, wittneben}@nari.ee.ethz.ch

***Abstract*—In this paper, we propose and investigate a low-complexity human motion tracking system which is based on ultra-wideband (UWB) radio nodes. The maximum likelihood (ML) solution of the localization problem that arises in such a system has been presented in [1]. However, the ML solution has a computational complexity that prohibits cost-effective real-time human motion tracking. In this paper, an iterative solution of the localization problem, which is based on the first order Taylor series (TS) approximation of the ranges between the anchors and the agents, is presented. The localization algorithm can handle range measurements with unknown offsets which arise due to the asynchronism between the clock of the agents and the anchors. By means of computer simulations, it is shown that the TS based approximate solution performs close to the ML solution within a few number of iterations if it is started with a "good" initial guess of the agents position. With the *a priori* knowledge of the agents trajectory and position estimates in the previous time-steps, the position in the next time-step can be predicted. It has been shown that using these predicted positions as an initial guess for the TS based approximation scheme greatly improves performance.**

I. Introduction

Human motion tracking has a wide range of applications in the fields ranging from medicine to virtual reality [2]. In clinical medicine, for example, it can be used to assist patients who undergo a stroke rehabilitation process [3]. Athletes performance can be improved by analyzing the data recorded during training. In virtual reality, motion tracking plays a vital role by feeding the action of the person (the user) to the computer in real-time [4]. Motion tracking systems are also employed in the film industry to record the motion of human and animal actors. The recorded information can then be used to animate fictional characters.

An "ideal" motion tracking system which meets the requirements of all the aforementioned applications should be [5]: 1) Accurate - estimate the position and orientation (pose) of different body parts with a very high precision; 2) Fast - update pose estimates at high frequency; 3) No line-of-sight (LOS) restriction - pose estimates should be immune to occlusion of different body parts [6]; 4) Robust - performance should not degrade due to external effects such as light, magnetic field and heat; and 5) Cheep.

Owing to the difficulty of finding such a "have-it-all" system that meets all the above requirements, there exist a variety of systems which are designed to suit to a specific application. The most prominent systems are those based on optical, inertial, magnetic sensing and time-of-flight based technologies (or a combination of them). Optical systems, which are based on cameras, provide accurate tracking with high sampling rate (e.g. [7], [8]). The main disadvantage of these systems is that they require dedicated infrastructure, complex setting, highly skilled operators and LOS restriction problem [9]. Inertial systems, which are based on accelerometers and gyroscopes, and magnetic systems (e.g. [2], [10]), on the other hand do not have LOS restriction but they are prone to drift errors and interference from near-by ferromagnetic materials.

For time-of-flight based systems electronic-textile (e-textile), which are fabrics that have interconnected electronic sensors and processors as an intrinsic part of the cloth, can be used [11]. Motion tracking such systems is either based on ultrasonic (e.g. [11]) or radio-wave propagation. For the latter case, one approach is motion tracking by means of ultra-wideband (UWB) radio communication, which is one of the most promising technologies for future body area networks [12], [13] . By exploiting the very large signal bandwidth (from 3.1 to 10.6 GHz) body mounted UWB nodes can determine their relative distance with very high spatio-temporal resolution and perform motion tracking based on this metric. Combined with the fact that such a system needs no external infrastructure, UWB positioning systems are particularly interesting for human motion tracking and can even be implemented as secondary application of an existing communication centric UWB body area network [1].

While UWB based human motion tracking systems may find application in several areas, substantial research is still required to prove its feasibility [14]. In [1], we have proposed a maximum likelihood (ML) positioning method for UWB based human motion tracking which takes into account the node topology constraints that are imposed by the kinematics of the body. Both simulation and experimental results assert that taking into account the node topology constraints alleviate the performance loss due to multipath propagation around the human body. Even if it has shown the feasibility of such a system, the ML solution has a computational complexity that prohibits cost-effective real-time human motion tracking.

Inspired by the results in [1], in this paper, we investigate an iterative solution of the localization problem which is based on the first order Taylor series (TS) approximation of the ranges between the anchors and the agents. The idea of this iterative scheme, which has the potential to greatly reduce the complexity of the tracking system, was first proposed in [15]. The scheme as presented there works only for the case when the range measurements have zero ranging offsets. However,

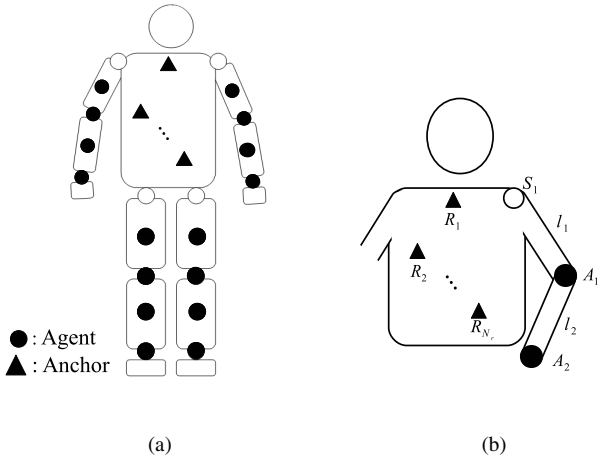

Fig. 1: (a) System setup. (b) Limb movement tracking.

for low complexity human motion tracking it is desired to have transmit-only agents which are not synchronized with the anchors. Owing to this fact, we have generalized the localization approach to handle ranging offsets that arise due to clock asynchronism between the agents and the anchors. In [15], it is stated that the localization algorithm almost always converges independently of the initial guess. However, based on simulation results, we show that if the initial guesses are not chosen carefully, the algorithm's convergence speed will be very slow, which would not allow real-time motion tracking. To circumvent this problem, we propose a method that provides good initial guesses by predicting the position of the agents from *a priori* knowledge of agents trajectory and estimates from previous time-steps.

The remainder of this paper is organized as follows. In Section II, we present the system setup that we are considering and define the localization problem that arises in such systems. The ML solution of the localization problem, for different clock synchronization cases, is then presented in Section III. The TS based approximate solution is then discussed in Section IV. In Section V, we discuss simulation results that assess the performance of both the ML solution and the TS based approximation.

II. System Setup and Problem Formulation

The general system setup that we consider is shown in Fig. 1(a). The anchors are attached on the fixed parts of the body (e.g. the torso) and are synchronized. The agents, on the other hand, are low complexity transmit-only nodes which are mounted on the body parts to be tracked. The agents may (or may not) be synchronized with each other and with the anchors.

With this system setup, tracking the movement of the limbs (arm or leg) corresponds to the localization problem shown in Fig 1(b). Herein $\{R_i\}_{i=1}^{N_r}$ represent the N_r anchor nodes (and also there position), $\{A_i\}_{i=1}^{N_a}$ denote the N_a agents (and also there position). The N_rN_a range measurements are denoted by $\hat{\boldsymbol{d}} = [\hat{d}_{11}, \ldots, \hat{d}_{N_rN_a}]^T$, where $\hat{d}_{ij}$ is the range measurement between anchor i and agent j.

The limb on which the agent A_i is located emanates from the joint located at position S_i (for e.g. the upper arm, on which agent A_1 is located, emanates from the shoulder joint located at S_1). The distance from joint S_i to agent A_i is denoted by l_i. In the spherical coordinate system, we note that S_i, A_i and l_i are related by

$$A_i = l_i \cdot [\cos\theta_i \sin\phi_i\,,\ \sin\theta_i \sin\phi_i\,,\ \cos\phi_i]^T + S_i \qquad (1)$$

where $[\theta_i, \phi_i]^T$ represents the orientation (azimuth and polar angles) of the ith limb. Hence, estimating the positions of the N_a agents corresponds to estimating the unknown parameter vector $\boldsymbol{\omega} \triangleq [\theta_1, \phi_1, \ldots, \theta_{N_a}, \phi_{N_a}]^T$.

In general, the range measurement between the ith anchor and the jth agent can expressed as

$$\hat{d}_{ij} = d_{ij} + e_{ij} + b_j, \qquad (2)$$

where $d_{ij} = \left\| \overrightarrow{R_iA_j} \right\|$ is the true distance between anchor i and agent j, e_{ij} is the range measurement error, and b_j is the range measurement offset due to the asynchronism between the clocks of the jth agent to that of the anchors. Hence, for the case when the agents are not synchronized with the anchors, the unknown (nuisance) ranging offsets need to be estimated along with the unknown parameter vector $\boldsymbol{\omega}$.

We consider four clock synchronization cases

1) *Synchronous*: all the agents are synchronized with the anchors. For this case, all the range measurement offsets are zero and known. Hence, we only need to estimate the unknown parameter vector $\boldsymbol{\omega}$.
2) *Group synchronous*: all the agents are synchronized with each other but not with the anchors. For this case, all the range measurement offsets are equal but unknown. Hence, along with $\boldsymbol{\omega}$, we need to estimate one unknown nuisance parameter.
3) *Partial group synchronous*: some of the agents form a group and agents which belong to a group share the same clock. This is a practically relevant scenario because it is easier to synchronize groups of agents (for example agents on the arm or agents on the leg) than synchronizing all the agents with each other. If there are N_g groups of agents, we need to estimate N_g unknown nuisance parameters along with $\boldsymbol{\omega}$.[1]
4) *Asynchronous*: the agents are synchronized neither with each other nor with the anchors. This is also a practically relevant scenario as it has the potential to greatly reduce the system complexity. For this case, we need to estimate N_a unknown nuisance parameters along with $\boldsymbol{\omega}$.

Hence, for the clock synchronization of case 2, 3 and 4 (which we collectively call the *non-synchronous cases* in the following), equation (2) can be re-written as follows

$$\hat{d}_{ij} = d_{ij} + e_{ij} + b_k, \text{ if } A_j \in \mathcal{G}_k,\ k \in \{1, 2, \ldots, N_g\}, \quad (3)$$

where $\mathcal{G}_k$ is the kth group of agents. We note that for the group synchronous case, $N_g = 1$ and $\mathcal{G}_1 = \{A_1, A_2, \ldots, A_{N_a}\}$. And for the asynchronous case, $N_g = N_a$ and $\mathcal{G}_k = \{A_k\}$.

[1]Note that $N_g \leq N_a$.

Define a vector $\boldsymbol{b} \triangleq \left[b_1, b_2, \ldots, b_{N_g}\right]^T$ which represents the unknown ranging offsets. With this formulation, the problem that we want to solve is the following: given the range measurements $\hat{\boldsymbol{d}}$, estimate $\boldsymbol{\omega}$ (for the synchronous case) or $\{\boldsymbol{\omega}, \boldsymbol{b}\}$ (for the non-synchronous cases) that fulfill the constraint in (1).

III. Maximum Likelihood Solution

In this section, we derive the maximum likelihood (ML) solution of the localization problem presented in Section II. We assume that the ranging errors are modeled as zero mean and statistically independent Gaussian random variables with variance σ_{ij}^2, i.e.

$$e_{ij} \sim \mathcal{N}\left(0, \sigma_{ij}^2\right).$$

ML solution for the synchronous case:

When the agents are synchronized with the anchors, the likelihood function of $\boldsymbol{\omega}$ takes the form [1]

$$p\left(\hat{\boldsymbol{d}} \middle| \boldsymbol{\omega} = \boldsymbol{\omega}'\right) = \prod_{j=1}^{N_a}\prod_{i=1}^{N_r} \frac{1}{\sqrt{2\pi\sigma_{ij}^2}} \exp\left(-\frac{\left(\hat{d}_{ij} - \left\|\overrightarrow{R_i A_j'}\right\|\right)^2}{2\sigma_{ij}^2}\right),$$

where x' represent the trial value of parameter x. Hence, the ML estimate of $\boldsymbol{\omega}$ is given by

$$\hat{\boldsymbol{\omega}} = \arg\min_{\boldsymbol{\omega}'} \sum_{j=1}^{N_a}\sum_{i=1}^{N_r} \frac{\left(\hat{d}_{ij} - \left\|\overrightarrow{R_i A_j'}\right\|\right)^2}{\sigma_{ij}^2}. \tag{4}$$

ML solution for the non-synchronous cases:

For the case when there is an asynchronism between the clock of the agents and the anchors, the ranging offsets $\boldsymbol{b}$ need to be estimated along with $\boldsymbol{\omega}$. The likelihood function of $\{\boldsymbol{\omega}, \boldsymbol{b}\}$ is given by [1]

$$p\left(\hat{\boldsymbol{d}} \middle| \boldsymbol{\omega} = \boldsymbol{\omega}', \boldsymbol{b} = \boldsymbol{b}'\right) = \prod_{k=1}^{N_g}\prod_{i=1}^{N_r}\prod_{j:\ A_j\in\mathcal{G}_k} \frac{1}{\sqrt{2\pi\sigma_{ij}^2}} \exp\left(-\frac{\left(\hat{d}_{ij} - \left\|\overrightarrow{R_i A_j'}\right\| - b_k'\right)^2}{2\sigma_{ij}^2}\right).$$

The joint ML estimate of $\{\boldsymbol{\omega}, \boldsymbol{b}\}$ then takes the form

$$\left\{\hat{\boldsymbol{\omega}}, \hat{\boldsymbol{b}}\right\} = \arg\min_{\boldsymbol{\omega}', \boldsymbol{b}'} \sum_{k=1}^{N_g}\sum_{i=1}^{N_r}\sum_{j:\ A_j\in\mathcal{G}_k} \frac{\left(\hat{d}_{ij} - \left\|\overrightarrow{R_i A_j'}\right\| - b_k'\right)^2}{\sigma_{ij}^2}. \tag{5}$$

Note that, since $\left\|\overrightarrow{R_i A_j}\right\|$ is a nonlinear function, the ML solutions in (4) and (5) are computationally demanding, and hence, not attractive for low-complexity real-time human motion tracking. In the next section, we present an iterative solution which circumvents this problem by linearizing $\left\|\overrightarrow{R_i A_j}\right\|$. But before we discuss the localization algorithm, we shall derive the optimum (ML) estimates of the ranging offsets in (5) which will be used in the iterative solution.

Optimum estimate of the ranging offsets:

For a given trial value of $\boldsymbol{\omega}'$ the ML estimate of the offsets can be computed analytically. We first note that for a given set of trial positions $\left\{A_j'\right\}_{j=1}^{N_a}$, which correspond to the trial orientations $\boldsymbol{\omega}'$, the cost function in (5) takes the following form [1]

$$\Psi(\boldsymbol{b}') = \sum_{k=1}^{N_g}\sum_{i=1}^{N_r}\sum_{j:\ A_j\in\mathcal{G}_k} \frac{(\psi_{ij} - b_k')^2}{\sigma_{ij}^2},$$

where $\psi_{ij} = \hat{d}_{ij} - \left\|\overrightarrow{R_i A_j'}\right\|$. Hence, the ranging offset of the kth group of agents that minimizes the cost function in (5) satisfies

$$\frac{\partial\Psi(\boldsymbol{b}')}{\partial b_k'} = 0$$
$$\Rightarrow \sum_{i=1}^{N_r}\sum_{j:\ A_j\in\mathcal{G}_k} \frac{(\psi_{ij} - b_k')}{\sigma_{ij}^2} = 0.$$

Thus, the optimum estimate of the kth group ranging offset that corresponds to the trial positions $\left\{A_j'\right\}_{j=1}^{N_a}$ is given by

$$b_k' = \frac{1}{\bar{\gamma}_k}\bar{d}_k - \frac{1}{\bar{\gamma}_k}\sum_{i=1}^{N_r}\sum_{j:\ A_j\in\mathcal{G}_k} \frac{\left\|\overrightarrow{R_i A_j'}\right\|}{\sigma_{ij}^2}, \tag{6}$$

where we have defined $\bar{\gamma}_k = \sum_{i=1}^{N_r}\sum_{j:\ A_j\in\mathcal{G}_k} 1/\sigma_{ij}^2$ and $\bar{d}_k = \sum_{i=1}^{N_r}\sum_{j:\ A_j\in\mathcal{G}_k} \hat{d}_{ij}/\sigma_{ij}^2$.

Note that for the group synchronous case, since we have only one group (and all agents belong to this group), the optimum estimate of the ranging offset takes the form

$$b' = \frac{1}{\bar{\gamma}}\bar{d} - \frac{1}{\bar{\gamma}}\sum_{i=1}^{N_r}\sum_{j=1}^{N_a} \frac{\left\|\overrightarrow{R_i A_j'}\right\|}{\sigma_{ij}^2},$$

with $\bar{\gamma} = \sum_{i=1}^{N_r}\sum_{j=1}^{N_a} 1/\sigma_{ij}^2$ and $\bar{d} = \sum_{i=1}^{N_r}\sum_{j=1}^{N_a} \hat{d}_{ij}/\sigma_{ij}^2$.

Similarly for the asynchronous case, the optimum estimate of the kth agent ranging offset is given by

$$b_j' = \frac{1}{\bar{\gamma}_j}\bar{d}_j - \frac{1}{\bar{\gamma}_j}\sum_{i=1}^{N_r} \frac{\left\|\overrightarrow{R_i A_j'}\right\|}{\sigma_{ij}^2},$$

with $\bar{\gamma}_j = \sum_{i=1}^{N_r} 1/\sigma_{ij}^2$ and $\bar{d}_j = \sum_{i=1}^{N_r} \hat{d}_{ij}/\sigma_{ij}^2$.

IV. Taylor-Series Approximation

In this section we present an iterative solution of the localization problem which is based on the first order TS approximation of $d_{ij} = \left\|\overrightarrow{R_i A_j}\right\|$. We first re-write (3) by replacing d_{ij} with its first order TS approximation. This will result in $N_r N_a$ simultaneous linear equations. The weighted least square solution of the system of equations is then presented.

The first order Taylor series expansion of $d_{ij} = \left\|\overrightarrow{R_i A_j}\right\|$ around a trial orientation $[\theta_i', \phi_i']^T$ is given by

$$d_{ij} \approx d_{ij}' + a_{ij}^{(\theta_i)}\delta_{\theta_i} + a_{ij}^{(\phi_i)}\delta_{\phi_i}, \tag{7}$$

where $a_{ij}^{(\theta_i)} = \frac{\partial d_{ij}}{\partial \theta_i}\Big|_{\theta_i', \phi_i'}$, $a_{ij}^{(\phi_i)} = \frac{\partial d_{ij}}{\partial \phi_i}\Big|_{\theta_i', \phi_i'}$, and $[\delta_{\theta_i}, \delta_{\phi_i}]^T$ is the difference between the true orientation and the trial orientation, i.e. $[\theta_i, \phi_i]^T = [\theta_i', \phi_i']^T + [\delta_{\theta_i}, \delta_{\phi_i}]^T$.

Note that for the synchronous case, plugging (7) into (3) results in the linear[2] equation

$$a_{ij}^{(\theta_i)} \delta_{\theta_i} + a_{ij}^{(\phi_i)} \delta_{\phi_i} \approx \hat{d}_{ij} - d'_{ij} - e_{ij}.$$

However, for the non-synchronous cases, the ranging offset needs to subtracted from the range measurement. Hence, we have the following linear equation

$$a_{ij}^{(\theta_i)} \delta_{\theta_i} + a_{ij}^{(\phi_i)} \delta_{\phi_i} \approx \hat{d}_{ij} - b'_k - d'_{ij} - e_{ij}, \text{ if } A_j \in \mathcal{G}_k \, .$$

The approach we propose to handle the unknown offsets in the range measurements is the following: For each trial orientation $[\theta_i', \phi_i']^T$, estimate the optimum offset b'_k using (6) and subtract it from the the range measurement.

Rewriting the system of $N_r N_a$ linear equations in matrix form, we get

$$\boldsymbol{\Gamma \delta} \approx \boldsymbol{z} - \boldsymbol{e}, \tag{8}$$

where we have defined the following matrices and vectors:

$$\boldsymbol{\Gamma} = \text{diag}\left\{\boldsymbol{\Gamma}_1, \boldsymbol{\Gamma}_2, \ldots, \boldsymbol{\Gamma}_{N_a}\right\},$$
$$\boldsymbol{e} = \left[e_{11}, e_{21}, \ldots, e_{N_r N_a}\right]^T,$$
$$\boldsymbol{\delta} = \left[\delta_{\theta_1}, \delta_{\phi_1}, \delta_{\theta_2}, \delta_{\phi_2}, \ldots, \delta_{\theta_{N_a}}, \delta_{\phi_{N_a}}\right]^T,$$
$$\boldsymbol{\Gamma}_i = \begin{bmatrix} a_{1i}^{(\theta_i)} & a_{1i}^{(\phi_i)} \\ a_{2i}^{(\theta_i)} & a_{2i}^{(\phi_i)} \\ \vdots & \vdots \\ a_{N_r i}^{(\theta_i)} & a_{N_r i}^{(\phi_i)} \end{bmatrix}, \; \boldsymbol{z} = \begin{bmatrix} \tilde{d}_{11} - d'_{11} \\ \tilde{d}_{21} - d'_{21} \\ \vdots \\ \tilde{d}_{N_r N_a} - d'_{N_r N_a} \end{bmatrix},$$

and $\tilde{d}_{ij} = \hat{d}_{ij}$ for the synchronous case, however, for the non-synchronous cases $\tilde{d}_{ij} = \hat{d}_{ij} - b'_k$ if $A_j \in \mathcal{G}_k$.

The weighted least squares solution of (8) is then given by

$$\hat{\boldsymbol{\delta}} = \arg\min_{\boldsymbol{\delta}} \left\| \boldsymbol{W}^{1/2} \left(\boldsymbol{z} - \boldsymbol{\Gamma \delta} \right) \right\|$$

where is $\boldsymbol{W}$ is an $N_r Na \times N_r N_a$ weighting matrix. For the case when the measurements are independent, $\boldsymbol{W}$ becomes a diagonal matrix, where each diagonal element represents the weight for the corresponding measurement. If the variance of the measurements are known, then the ideal weight for each measurement is the reciprocal of the variance. This is intuitive because the weighting makes sure that good measurements are emphasized while bad measurements are deemphasized.

Since the the range measurements are independent, we note that the weighted least squares solution of (8) takes the form [15]

$$\hat{\boldsymbol{\delta}} = \left(\boldsymbol{\Gamma}^T \boldsymbol{\Sigma}^{-1} \boldsymbol{\Gamma} \right)^{-1} \boldsymbol{\Gamma}^T \boldsymbol{\Sigma}^{-1} \boldsymbol{z}, \tag{9}$$

where $\boldsymbol{\Sigma} = \text{diag}\left\{\sigma_{11}^2, \ldots, \sigma_{N_r N_a}^2\right\}$ is the covariance matrix of the range measurements.

The localization algorithm then works as follows

1) Choose an initial guess of the agents orientation $\left\{[\theta_i', \phi_i']^T\right\}$.
2) Approximate $\left\{\left\|\overrightarrow{R_i A_j}\right\|\right\}$ around $\left\{[\theta_i', \phi_i']^T\right\}$ with its first order TS expansion and determine the matrix $\boldsymbol{\Gamma}$ in (8).
3) For the non-synchronous cases, subtract the optimum ranging offset estimate using (6) from the range measurement to result in $\tilde{d}_{ij} = \hat{d}_{ij} - b'_k$. However, for the synchronous case, $\tilde{d}_{ij} = \hat{d}_{ij}$.
4) Calculate $\boldsymbol{z}$.
5) Estimate $\boldsymbol{\delta}$ using (9).
6) Update the orientations using the newly estimated $\hat{\boldsymbol{\delta}}$, i.e. $\theta_i' \leftarrow \theta_i' + \hat{\delta}_{\theta_i}$ and $\phi_i' \leftarrow \phi_i' + \hat{\delta}_{\phi_i}$.
7) If $\boldsymbol{\delta}$ is above a threshold value, go back to 2.
8) $\left\{[\theta_i', \phi_i']^T\right\}$ are the orientation estimates.

Note that the weighted least squares solution in (9) only requires the covariance matrix of the range measurement errors but it does not assume any distribution. Hence, the localization algorithm works for range measurements taking any type of distribution. In [15], it has been stated that the algorithm converges almost always independently of the chosen initial guess. In the next section, we will show that for not carefully chosen initial guesses the algorithm converges very slowly.

V. Simulation-Based Performance Analysis

In this section, we discuss simulation results that assess the performance of the localization algorithms presented in Sections III and IV. For all the simulations, four anchors were mounted on the torso at locations $R_1 = [-15\,\text{cm}, 0, 5\,\text{cm}]^T$, $R_2 = [-25\,\text{cm}, 20\,\text{cm}, 0]^T$, $R_3 = [-5\,\text{cm}, 20\,\text{cm}, 0]^T$ and $R_4 = [-15\,\text{cm}, 40\,\text{cm}, 15\,\text{cm}]^T$.[3] Two agents were mounted at the left arm (one at the elbow joint and the other one at the wrist joint). The length of the upper arm and the forearm is set to 30 cm. The standard deviation of all the ranging errors is the same and is set to $0.3612\,\text{cm}$ (which corresponds to a variance of $0.1\,\text{cm}^2$).

Figure 2 shows the cumulative density function (CDF) of the root mean squared error (RMSE) of both the ML solution and the TS based approximate solution. The initial guess for the TS based approximate solution is chosen randomly and the maximum number of iterations is set to 100. Figure 2(a) shows the CDF plots of the RMSE of the *elbow position* estimates. From the figure, we first note that for all the clock synchronization cases – synchronous (black lines), group synchronous (green lines) and asynchronous (yellow lines) – the TS based approximate solution performs reasonably close to its ML counter part.

The other point we note in Figure 2(a) is that for both localization techniques, the synchronous case performs better than the group synchronous case which in turn outperforms the asynchronous case. For the ML estimator, the result is very intuitive because we have to estimate one more variable in the group synchronous case (and N_a more variables in the

[2]Linear with respect to the unknown variables δ_{θ_i} and δ_{ϕ_i}.

[3]The left shoulder joint is chosen as the center of the coordinate system.

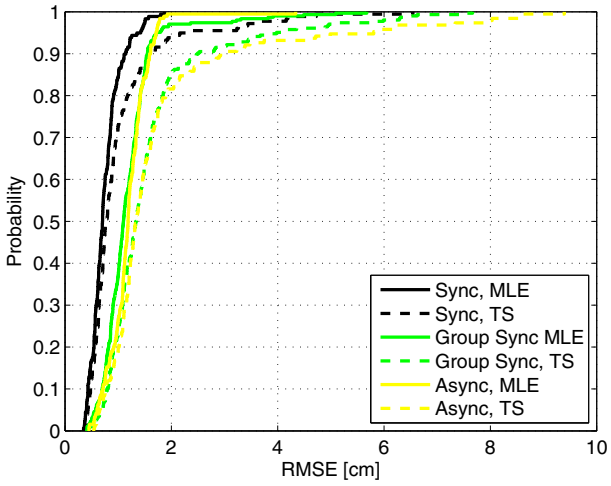

(a) Elbow

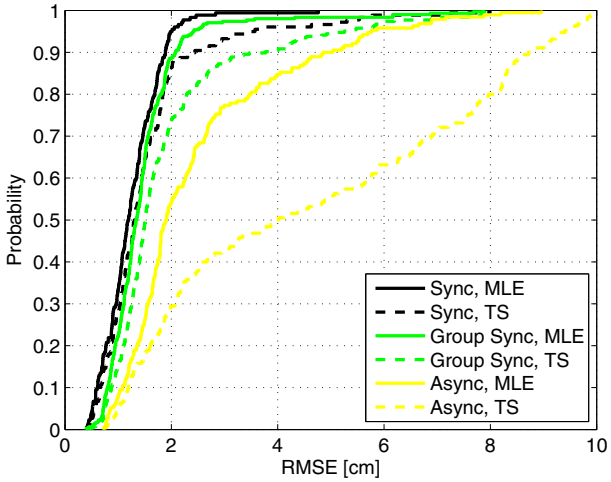

(b) Wrist

Fig. 2: CDF plot of the RMSE of the ML estimator and TS based approximation with 100 iteration and random initial guess.

asynchronous case) as compared to that of the synchronous case. Similarly, for the TS based approximate solution, we use the estimates in (6) to suppress the offset in the range measurements. Since the offset estimates are not perfect, a performance loss is expected in the non-synchronous cases as compared to the synchronous counter part. We further note that since the offset estimate in the group synchronous case uses $N_r N_a$ range measurements, it is more accurate than that of the asynchronous case which uses only N_r range measurements to estimate the offset for each agent.

The CDF plot of the RMSE of the *wrist position* estimates is shown in Figure 2(b). We first note that for all the synchronization cases, the wrist position estimates are worse than the elbow position estimates. This is expected because the elbow is connected to the shoulder joint which has a fixed and known position, however, the wrist is connected with the elbow joint whose position has to be estimated.

From Figure 2(b), we further note that the estimates of the TS based approximation perform poorly as compared to the ML estimates. This poor performance of the TS based approximation is attributed to the random initial guesses and the restriction on the maximum number of allowed iterations (which is set to 100). If we let the algorithm iterate until a target accuracy is achieved, the TS based solution would have performed close to the ML solution. However, for real-time human motion tracking, the position of the agents has to be updated with a certain frequency, which means that we have a restriction on the maximum allowed number of iterations. If, on the other hand "good" initial guesses are used, the algorithm achieves the target accuracy with few iterations.

Figure 3 shows the CDF plot of the RMSE of the wrist position estimates using the TS approximation for the asynchronous case. Shown in the figure are estimates using true agent position as an initial guess (blue solid line) and estimates with random initial guess (yellow dotted lines). The number of iterations for both cases is set to 100. We note that a substantial performance gain is achieved when the initial guesses are chosen appropriately.

Next we shall discuss the performance improvement that can be achieved by the TS based approximation when we predict the position of the agents from *a priori* knowledge of the agents trajectory and estimates from the previous time-step, and then use this predicted positions as an initial guess in the next time-step.

Consider the scenario which is shown in Figure 4. The wrist follows the trajectory which is marked with "□". For clarity reason, what is shown in the figure are the positions after 3 time-steps, i.e. between two plotted position there are three more position updates. In most of the human actions (for e.g. walking), the average speed of different limbs movement can be estimated. Furthermore, the update frequency of the motion tracking system is known. Equipped with the knowledge of the system update rate and the average speed of the limb's

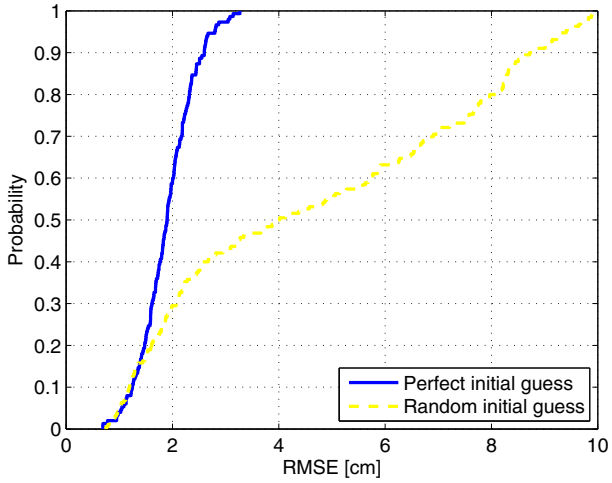

Fig. 3: CDF plot of the RMSE of the TS based approximate solution at the 100th iteration with perfect initial guess and random initial guess.

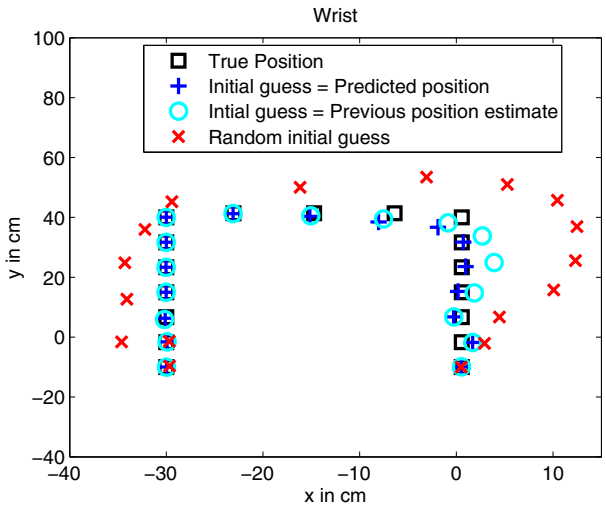

Fig. 4: Wrist movement tracking: Position estimates of the TS based approximation at the 100th iteration using different initial guesses.

movement, distance between the position of the wrist between two time-steps can be estimated. In the simplest case, with *a priori* knowledge of the agents trajectory as given in the figure, the position of the agent in the next time step can be determined from the estimate in the current time-step.

Figure 4 also shows the estimates of the TS based approximation at the 100th iteration for different initial guesses. We note that using random initial guess it is not possible to accurately follow the trajectory of the wrist with only 100 iterations. However, if we carefully chose the initial guess good enough positioning accuracy can be achieved. It is worthwhile to note that the estimates which use the position estimates from previous time-steps are very close to that of the estimates which use the predicted positions as their initial guess. Hence, if the system can afford fast update rates (which is the case for UWB based motion tracking systems) taking position estimates from previous time step will greatly improve performance.

VI. Conclusion

In this paper, we have presented a low-complexity UWB radio based human motion tracking system. An iterative solution of the localization problem that arise in such a system, which is based on first order TS approximation, has been discussed. It was shown that for the case when the clock of the agents and the anchors are synchronized with each other, the iterative solution preforms close to the ML solution. However, for the case when the agents are not synchronized with the anchors, which is the practically preferred approach as it has the potential to reduce the system complexity, the convergence speed of the localization algorithm heavily depends on the chosen initial guess. Predicting the agents position from previous time-step estimates and using them as an initial guess for the estimation in the next time-step has been shown to greatly improve localization performance.

References

[1] Z. W. Mekonnen, E. Slottke, H. Luecken, C. Steiner, and A. Wittneben, "Constrained maximum likelihood positioning for UWB based human motion tracking," in *2010 Int. Conf. on Indoor Pos. and Indoor Nav.*, 2010.

[2] R. Zhu and Z. Zhou, "A real-time articulated human motion tracking using tri-axis inertial/magnetic sensors package," *IEEE Tran. on Neu. Sys. and Rehab. Eng.*, vol. 12, no. 2, pp. 295–302, Jun. 2004.

[3] H. Zheng, N. Black, and N. Harris, "Position-sensing technologies for movement analysis in stroke rehabilitation," *Medical and Biological Engineering and Computing*, vol. 43, pp. 413–420, 2005, 10.1007/BF02344720.

[4] H. Zhou and H. Hu, "A survey - human movement tracking and stroke rehabilitation," University of Essex, Tech. Rep., Dec. 2004.

[5] J. Richards, "The measurement of human motion: A comparison of commercially available systems," *Proc. Fifth Int'l Symp. 3D Analysis of Human Movement*, 1999.

[6] G. Welch and E. Foxlin, "Motion tracking: No silver bullet, but a respectable arsenal," *IEEE Comp. Graphics and App.*, vol. 22, no. 6, pp. 24–38, Dec. 2002.

[7] R. Poppe, "Vision-based human motion analysis: An overview," *Computer Vision and Image Understanding*, vol. 108, no. 1-2, pp. 4–18, 2007, special Issue on Vision for Human-Computer Interaction.

[8] J. K. Aggarwal and Q. Cai, "Human motion analysis: A review," *Computer Vision and Image Understanding*, vol. 73, no. 3, pp. 428–440, 1999.

[9] H. A. Shaban, M. A. El-Nasr, and R. M. Buehrer, "Toward a highly accurate ambulatory system for clinical gait analysis via UWB radios," *IEEE Transactions on Information Technology in Biomedicine*, vol. 14, no. 2, pp. 284 –291, 2010.

[10] J. Hol, F. Dijkstra, H. Luinge, and T. Schon, "Tightly coupled UWB/IMU pose estimation," in *IEEE International Conference on Ultra-Wideband, 2009. ICUWB 2009.*, 2009, pp. 688 –692.

[11] C. Einsmann, M. Quirk, B. Muzal, B. Venkatramani, T. Martin, and M. Jones, "Modeling a wearable full-body motion capture system," *Ninth IEEE International Symposium on Wearable Computers, 2005*, pp. 144–151, Oct. 2005.

[12] L. Yang and G. B. Giannakis, "Ultra-wideband communications: an idea whose time has come," *IEEE Signal Processing Magazine*, vol. 21, no. 6, pp. 26–54, Nov. 2004.

[13] H. Cao, V. Leung, C. Chow, and H. Chan, "Enabling technologies for wireless body area networks: A survey and outlook," *IEEE Communications Magazine*, vol. 47, no. 12, pp. 84–93, Dec. 2009.

[14] M. Di Renzo, R. Buehrer, and J. Torres, "Pulse shape distortion and ranging accuracy in UWB-based body area networks for full-body motion capture and gait analysis," *IEEE Global Telecommunications Conference, 2007. GLOBECOM '07.*, pp. 3775–3780, Nov. 2007.

[15] W. Foy, "Position-location solutions by Taylor-series estimation," *IEEE Tran. on Aero. and Elec. Sys.*, vol. AES-12, no. 2, pp. 187–194, 1976.